Vietnam Journal of Catalysis and Adsorption
Tạp chí xúc tác và hấp phụ Việt Nam

https://jca.edu.vn/

An insight into characteristics of nonconventional hydrogen bonds in the complexes of haloforms with carbon monoxide

Le Thi Tu Quyen[1], Nguyen Van Hien[1], Vo Van Quan[2], Vu Thi Ngan[1], Nguyen Tien Trung[1,*]

[1] *Laboratory of Computational Chemistry and Modelling (LCCM), Faculty of Natural Sciences, Quy Nhon University, 170 An Duong Vuong Street, Binh Dinh province 55000, Viet Nam*
[2] *The University of Danang - University of Technology and Education, Danang 550000, Vietnam*
** Email: nguyentientrung@qnu.edu.vn*

ARTICLE INFO

Received: 23/05/2025
Accepted: 07/06/2025
Published: 30/06/2025

Keywords:
nonconventional hydrogen bond; blue shift; intermolecular distance; SAPT2+

ABSTRACT

The interaction between X_3CH (X=F, Cl, Br) and CO were investigated through *ab initio* methods. The stability of complexes and their nonconventional C-H···O hydrogen bond decreases as the C-H polarity in haloform declines in the order Br_3CH > Cl_3CH > F_3CH. The C-H blue shift of C-H···O hydrogen bonds increases from F_3CH···OC to Br_3CH···OC due to the decreasing occupation at antibonding σ*(C-H) orbitals when X goes from F to Br. The formation of C-H···O hydrogen bonds in X_3CH···OC are found at the intermolecular C···O distance from 2.9 to 3.7 Å. The C-H blue shift decreases as the intermolecular distance between monomers increases. Remarkably, the significant contribution of dispersion component is observed along with the decreasing C-H blue shift at the equilibrium C···O distance region of 3.3-3.7 Å. The SAPT2+ analysis reveals a dominant contribution of dispersion and electrostatic components to complex stabilization, with the dispersion term playing a larger role.

Introduction

The hydrogen bond A-H···B is a non-covalent interaction that plays an important role in numerous scientific fields [1-7]. It not only determines the structure of biological macromolecules, such as DNA, RNA and protein but also causes solvation, the physical absorption on surfaces and contributes to the biochemical processes [8-10]. The essential role of H-bond is also displayed in supramolecular synthesis, crystal design and packing.[11-13] In addition, the presence of hydrogen bonds also contributes to form self-healing polymer and influence on the mechanism [14,15]. For example, the formation of hydrogen bond between nitrosobenzene (PhNO) and carboxylic acid can promote the reduction of PhNO [15].

Normally, the formation of the H-bond is due to an electrostatic interaction between H and B atoms, leading to an elongation of the A-H distance and a decrease in its stretching frequency as compared to the original A-H monomer. This type of hydrogen bond is conventionally referred to as a red-shifting hydrogen bond [16]. Until in 1980, Sandofy and his co-workers discovered a new hydrogen bond called a blue-shifting hydrogen bond, which is characterized by a contraction of A-H bond length along with an increase in its stretching frequency [17]. The blue-shifting hydrogen bond has been revealed in systems where a hydrogen atom is bonded to a carbon atom and forms a hydrogen bond with either an electronegative atom or a region having an excess electron density [18]. The appearance of blue-shifting

https://doi.org/10.62239/jca.2025.023

hydrogen bonds has opened many interesting ideas for scientists to shed light on their characteristics. Through many years of research, scientists have obtained many results around the nature of blue-shifting hydrogen bonds in many systems, and among them, hydrogen bonds in haloform systems gave meaningful results in both theory and experiment. Indeed, in 1997, Boldeskul reported experimental results about the blue shift of the C-H/D bond involving the hydrogen bonds in complexes of haloform with different proton acceptors in solution [19]. Hobza's research team also observed the agreement between experimental and theoretical results when studying the anti-hydrogen bond between chloroform and fluorobenzene [20]. In addition, a theoretical prediction for the blue shift of the C-H···O hydrogen bond at 47 cm^{-1} had been suggested before in the CHF_3···CH_3OH complex at the MP2/6-311+G(d,p) level of theory [21] Therefore, these publications contributed to establishing the basis for several theoretical studies on the blue-shifting hydrogen bonds in the interactions containing haloform. [22-26] For example, a C-H blue shift of 41 cm^{-1} in the CHX_3···HNO complexes (X= F, Cl, Br) was obtained at MP2/6-311++G(d,p) level [22] Another study by Gopi et al. showed a good agreement between an experimental blue shift of C-H in C-H···O hydrogen bonds with computed one calculated at MP2/6-311++G(d,p) in CHF_3···H_2O complex. Therein, the C-H bond is blue-shifted by 20.3 and 32.3 cm^{-1} in argon and neon matrices, respectively. Meanwhile, the theoretical result for the C-H blue shift is 39.4 cm^{-1}. The difference between the experimental and theoretical results is due to the interaction of environmental factors (argon and neon) to complex [23]. Although the characteristics of blue-shifting hydrogen bonds have been revealed through many efforts of scientists, their origin still remains unanswered. Thus, extending research into the blue shift of nonconventional hydrogen bonds involving C_{sp3}-H as a proton donor is particularly necessary to clarify the origin of this type of hydrogen bond.

Up to now, studies on the interactions related to CO or CO_2 molecules have been extremely significant because of their contribution to solving environmental problems as well as giving various models to explain the characteristics of blue-shifting hydrogen bonds. In 2011, Roman Szostak pointed out that the characteristics of hydrogen bonds in the interaction between the X-H bond (X= O, N, C, S, Se, P, S, B, F, Cl, Br) and CO_2 depend on the charge on H atom of the isolated proton donors. Specifically, the blue shift is observed when the positive charge on the H atom is small, in contrast, the more positive charge on the H atom leads to the red-shifting [27]. Trung and his co-workers had a different approach, that explained the formation and nature of hydrogen bond based on initial properties of isolated monomers. Therein, the polarity of proton donors, which is evaluated via the deprotonation enthalpy (DPE), and proton affinity (PA) at proton acceptors display a close relationship with the blue or red shift of hydrogen bonds [28-31] Especially, the ratio of DPE/PA was also used as a factor to classify the characteristics of hydrogen bonds [29].

The C-H···O blue-shifting hydrogen bonds in the interactions of CHF_3, $CHCl_3$ with CO_2, H_2O and CO molecules were reported [32,33]. Nevertheless, the systematic study of the stability of complexes, strength and nature of hydrogen in the complexes of haloform and CO have not been reported. Therefore, we investigate the role of different X substitutions on the polarity of C-H proton donors that can cause considerable impact on the strength of complexes and the characteristic of C-H···O hydrogen bonds in the complexes of the X_3CH (X= F, Cl, Br) with CO molecule using quantum chemistry approaches. Furthermore, the different distances between the C atom of the proton donors and the O atom of the proton acceptor are fixed to investigate the effect of the C···O distance on the complex stabilization and the characteristics of the hydrogen bonds. The obtained results help to shed light on the nature of blue-shifting H-bonds and the contribution of energy components to the stability of complexes and the nature of C-H···O hydrogen bonds.

Theoretical methods

The calculation for geometrical optimization of monomers and complexes, and harmonic vibrational frequency in the system between X_3CH (X= F, Cl, Br) and CO is carried out at MP2/6-311++G(3df,2pd) level of theory by Gaussian 09 program [34]. Interaction energy with corrections of zero-point energy (ZPE) and basis set superposition errors (BSSE) using the Boys and Bernardi scheme are calculated at the same level of theory [35].

The formation and strength of hydrogen bonds are investigated using Atom in Molecule (AIM) analysis [36] at the MP2/6-311++G(3df,2pd) level. Indeed, electron density (ρ(r)) at bond critical points (BCPs) is computed by means of the AIMALL program [37]. The Individual energy of each hydrogen bond (E_{HB}) is evaluated by the formula of Espinosa-Molins-Lecomte: E_{HB} = 0.5V(r),

https://doi.org/10.62239/jca.2025.023

in which V(r) is the electron potential energy density.[38] Hyperconjugation energies and change of electron density on anti-bonding orbitals are obtained from the Natural Bond Orbitals (NBO) analysis by means of the NBO 5.0 program [39].

SAPT2+ analysis [40] was carried out at 6-311++G(3df,2pd) basis set for calculating energy components contributing to the complex stability and classification of C-H···O hydrogen bond in the complexes. The interaction energy in SAPT2+ analysis is calculated as the following equation:

$$\Delta E_{SAPT} = E_{ele} + E_{exc} + E_{ind} + E_{dis} + \delta E_{int}^{HF}$$

In which, E_{ele}, E_{exc}, E_{ind} and E_{dis} are electrostatic, exchange, induction, and dispersion energy terms, respectively. The δE_{int}^{HF} is the total energy of the third and higher level of induction and exchange components.

Results and discussion

Geometries and AIM analysis

The geometrical optimization of the $X_3CH\cdots OC$ (X = F, Cl, Br) complexes at the MP2/6-311++G(3df,2pd) level induces three stable complexes on the potential energy surface with similar geometrical structures as shown in Fig 1. All complexes belong to the C_{3v} symmetry point group, which includes one weak C-H···O interaction. The intermolecular distances O···H ($R_{O...H}$) ranging from 2.38 to 2.56 Å are smaller than the sum of Van der Walls radii of O and H atoms (2.72 Å). This observation leads to a prediction for the formation of C-H···O hydrogen bonds between monomers following complexation.

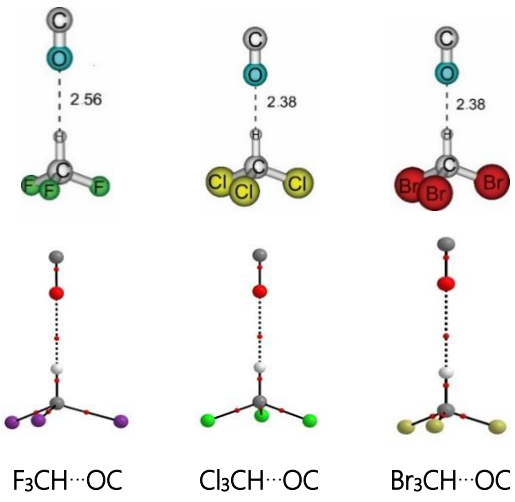

Fig 1. Stable structures and topological geometry of complexes $X_3CH\cdots OC$ (X =F, Cl, Br)

The results from AIM analysis, however, immediately confirm the existence of the C-H···O hydrogen bonds in investigated complexes through the appearance of bond critical point (BCP) between interacted atoms H and O. Therein, the electron density values ρ(r) and Laplacian of the electron density $\nabla^2(\rho(r))$ at these BCPs, which are shown in Table 1, are in the range of 0.0066 – 0.0088 (au) and 0.024 – 0.0529 (au), belonging to the region of the hydrogen bond formation (ρ(r) = 0.002 – 0.035 au, and $\nabla^2(\rho(r))$ = 0.02 – 0.15 au) [41]. This observation is proved by the individual energies (E_{HB}) of the C–H···O hydrogen bonds take negative values from -5.0 to -7.8 kJ.mol^{-1} as given in Table 1.

Notably, the E_{HB} values of C-H···O hydrogen bonds are more negative when X goes from F to Cl and Br, demonstrating an increase in the strength of the C–H···O hydrogen bond in the order of complexes $F_3CH\cdots OC$ (E_{HB} = -5.0 kJ.mol^{-1}) < $Cl_3CH\cdots OC$ (E_{HB} = -7.8 kJ.mol^{-1}) ~ $Br_3CH\cdots OC$ (E_{HB} = -7.8 kJ.mol^{-1}).

Table 1. Interaction distance of C···O ($R_{C...O}$, Å) and O···H ($R_{O...H}$, Å), deprotonation enthalpy of C-H bond (DPE, kJ.mol^{-1}) in the isolated monomers, electron density (ρ(r), au), Laplacian electron density ($\nabla^2(\rho(r)$, au) at BCP, and individual energy of hydrogen bond (E_{HB}, kJ.mol^{-1}) in $X_3CH\cdots OC$ complexes (X =F, Cl, Br)

	$F_3CH\cdots OC$	$Cl_3CH\cdots OC$	$Br_3CH\cdots OC$
$R_{C\cdots O}$ (Å)	3.64	3.47	3.49
$R_{O...H}$ (Å)	2.56	2.38	2.38
ρ(r) (au)	0.0060	0.0088	0.0088
$\nabla^2(r)$ (au)	0.0236	0.0350	0.0352
E_{HB} (kJ.mol^{-1})	-5.0	-7.8	-7.8
DPE (kJ.mol^{-1})	1595.7	1514.8	1483.8
DPE (kJ.mol^{-1}) (experiment)	1582.0±5.9*	1507.6*	1463.0±9.2*

*Experimental values taken from the NIST webpage

This tendency can be explained by an enhancement of the C-H polarity in the isolated monomers in the sequence of F_3CH < Cl_3CH < Br_3CH. Indeed, the DPE values of C-H bond in the F_3CH, Cl_3CH and Br_3CH monomers are in turn 1595.7, 1514.8 and 1483.8 kJ.mol^{-1} (*cf.* Table 1). Therefore, the strength of the C-H···O hydrogen bonds increases along with the polarity of the C-H proton donors in the isolated monomers. The study by Man et al. on the complexes of X_3CH with NH_2Y (X, Y= F, Cl, Br) at MP2/6-311++G(d,p) also showed an increase in both the strength of the C-H···N hydrogen bonds and polarity of C-H bonds when X turns from F to Cl and then Br [29].

To evaluate the effects of the distance between proton donors and proton acceptors on the formation and stability of complexes as well as the C-H···O hydrogen bonds, we optimize geometrical structures of X_3CH···OC complexes by fixing the distance between the C atom of X_3CH and the O atom of the CO at MP2/6-311++G(3df,2dp) level. This distance varied in the range of 2.7 to 4.5 with increments of 0.2 Å. The results show 30 structures with the same geometry and C_{3v} molecular symmetry.

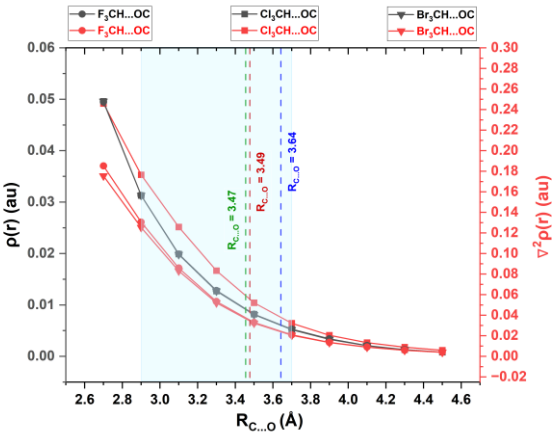

Fig 2. The relationship between electron density ρ(r) (au) and Laplacian electron density $\nabla^2(\rho(r))$ (au) at BCPs as fixing C···O distance ($R_{C...O}$, Å) in X_3CH···OC complexes (X= F, Cl, Br)

The topological geometry analysis of stable complexes points out that the complexation is due to the C-H···O interactions. The intermolecular distances C···O ($R_{C...O}$) and topological parameters at BCPs are shown in Table S1 of Supporting Information (SI). The relationship between intermolecular distance C···O ($R_{C...O}$) and electron density ρ(r) and Laplacian of electron density $\nabla^2(\rho(r))$ of C-H···O hydrogen bonds are presented in Fig 2. The obtained results show that at the intermolecular distance of C···O from 2.9 to 3.7 Å, the formation of C-H···O hydrogen bonds in X_3CH···OC complexes are observed with the values of ρ(r) and $\nabla^2(\rho(r))$ are in the ranges of 0.0033 – 0.0313 au, and 0.0205 – 0.1306 au, respectively. Additionally, the values of electron energy density H(r) are also positive at the region of $R_{C...O}$ = 2.9–3.7 Å. Remarkably, the $R_{C...O}$ = 2.9 – 3.7 Å also includes the equilibrium structures of F_3CH···OC, Cl_3CH···OC and Br_3CH···OC, with equilibrium $R_{C...O}$ distance in turn 3.64, 3.47 and 3.49 Å.

Interaction energies

The interaction energies of investigated complexes corrected both ZPE and BSSE (ΔE^*) are computed at MP2/6-311++G(3df,2pd) level of theory to evaluate the stability of X_3CH···OC complexes. The result provides that the ΔE^* values are -0.6, -2.1 and -2.5 kJ.mol^{-1} for F_3CH···OC, Cl_3CH···OC and Br_3CH···OC, respectively. These values indicate that the geometrical structures of complexes are quite stable on the potential energy surface.

The stability of X_3CH···OC complexes are weaker than that of X_3CH···NH_3 (X= F, Cl, Br) with their ΔE^* values ranging from -12.3 to -15.9 kJ.mol^{-1} calculated at CCSD(T)/6-311++G(3df,2pd)//MP2/6-311++G(d,p) level of theory.[29] It can be due to proton affinity at O in CO being just nearly half that at N in NH_3. Indeed, the PA values are 852 kJ.mol^{-1} for NH_3 [29] and 416 kJ.mol^{-1} for CO. In addition, the strength of complexes increases upon the substitutions of X in the order of F < Cl < Br, being consistent with a decrease of individual energy of the C-H···O hydrogen bond obtained in AIM analysis. The increase in the stability of complexes as X to be F and Cl was stated in X_3CH···OH_2 (X= F, Cl) complexes by Zierkiewicz [42] With the higher level computational theory used in the present work, it is also shown that the stability of X_3CH···OC (X= F, Cl, Br) complexes is enhanced from X to Cl, and then to Br. In addition, In the comparison with the H_2O···OC complex, its interaction energy calculated at MP2/6-311++G(3d,3p) is 7.0 kJ.mol^{-1} more negative than, that of X_3CH···OC complexes [43] This shows the higher strength of both the H_2O···OC complex compared to X_3CH···OC and conventional O-H···O hydrogen bond in the former relative to the nonconventional C-H···O hydrogen bonds in the latter.

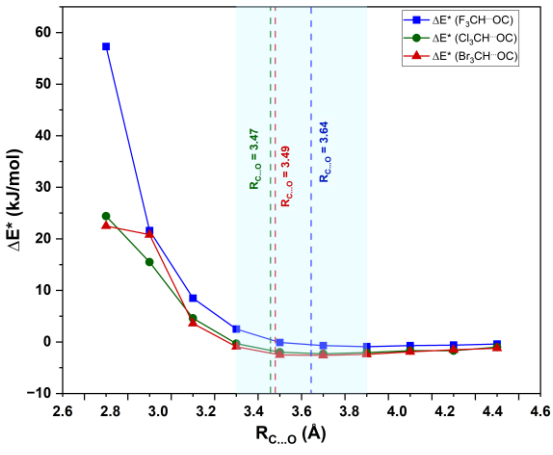

Fig 3. Interaction energy (ΔE^*, kJ.mol^{-1}) as fixing intermolecular distances of C···O ($R_{C...O}$, Å) in the complexes X_3CH···OC (X = F, Cl, B)

The dependence of interaction energies of the complexes on the C···O intermolecular distance is illustrated in Fig 3. The results show that complexes are

the most stable on their potential energy surface when $R_{C...O}$ values are in the range of 3.3–3.9 Å. Remarkably, the complexes get positive interaction energy values at $R_{C...O}$ = 2.7–3.1 Å, indicating that complexes are not stable at close C···O intermolecular distances. This assessment is reasonable as the close intermolecular distance can induce a repulsive force, thus reducing the stability of complexes. Similarly, when $R_{C...O}$ value passes over the region of 3.3–3.9 Å, the stability of complexes also decreases because of the intermolecular contact becoming further. For the same $R_{C...O}$ values, the stability of complexes also increases in the sequence of the isolated monomer of F_3CH < Cl_3CH < Br_3CH. This observation agrees well with the stability tendency of X_3CH···OC complexes at their equilibrium geometrical structures.

Changes in C-H bond lengths and their stretching frequencies

The changes in C–H bond lengths (Δr), their stretching frequency (Δν) and selected data from NBO analysis in the complexes are calculated at MP2/6-311++G(3df,2pd) level. The negative values Δr from -0.0013 to -0.0006 Å, and Δν being positive from 17.3 to 30.7 cm^{-1} demonstrate a contraction of the C-H bond lengths and an increase in its stretching frequency upon the complex formation. Therefore, the C-H stretching frequency involving C-H···O hydrogen bonds is characterised by the blue shift. The C-H contractions in X_3CH···OC complexes in this work are found to be more considerable than those in X_3CH···NH_3 ones reported by Man *et al.* [29]. This should be due to the larger proton affinity at N of NH_3 compared to that at O of CO.

Moreover, the comparison of Δr(C-H) values between complexes of Cl_3CH and CO, SO_2 and NH_3 points out that Δr(C-H) values in the complexes of Cl_3CH is raised from CO to SO_2, [32] and then NH_3.[29] This trend is in an agreement with the increase of proton affinity from CO to SO_2 and then NH_3. Indeed, the experimental PA value of CO, SO_2 and NH_3 is 426.3 $kJ.mol^{-1}$, 672.3 $kJ.mol^{-1}$[32] and 853.6 $kJ.mol^{-1}$ [29], respectively. Notably, the changes in the stretching frequency of the C-H bond of F_3CH···OC, Cl_3CH···OC and Br_3CH···OC are in turn 17.3, 30.7 and 30.4 cm^{-1}. Therefore, the magnitude of blue shift of C-H stretching frequency involving C-H···O hydrogen bonds in investigated complexes is enhanced when X goes from F to Cl and Br. This result is explained by a larger decrease in the electron density at antibonding σ^*(C-H) orbital of Cl_3CH···OC (-0.0012 e) and Br_3CH···OC (-0.0009 e) as compared to that in of F_3CH···OC (-0.0004 e). The second-order perturbation energy (E(2)) for the intermolecular electron density transfer from lone pairs at O atom (n(O)) to antibonding σ^*(C-H) orbital (n(O) → σ^*(C-H)) is in the range of 1.2 to 1.3 $kJ.mol^{-1}$, indicating the effect of a weak hyperconjugative interaction to the blue-shifting in the C-H stretching frequency. This observation is similar to the report of Alagubin when evaluating the effects of factors including hyperconjugative interaction, rehybridization and repolarization of A-H bond to hydrogen bond classification [44] Moreover, the E(2) of n(O) → σ^*(C-H) electron transfer increase in the order of X: F (1.1 $kJ.mol^{-1}$) < Cl (1.2 $kJ.mol^{-1}$) < Br (1.3 $kJ.mol^{-1}$), being consistent with the strength tendency of C-H···O hydrogen bond upon the changing of X.

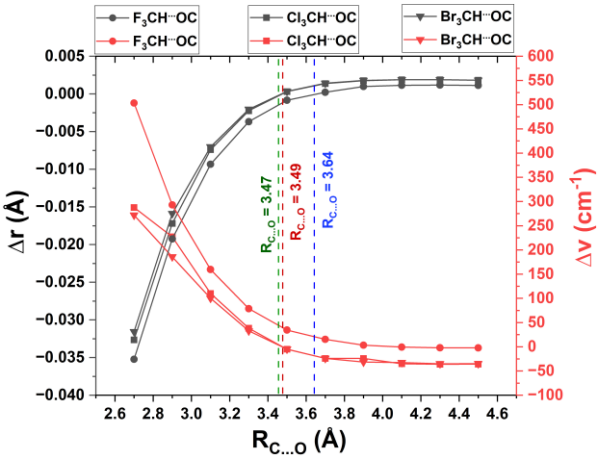

Fig 4. The relation between changes of C-H bond lengths (Δr, Å) and their stretching frequencies (Δν, cm^{-1}) with the changes of C···O distances ($R_{C...O}$, Å)

In order to evaluate the influence of C···O intermolecular distance on the blue-shift or red-shift of the C-H stretching frequency, the changes in the C-H bond lengths and its stretching frequency according to the variation of C···O distance are calculated and collected in Table S2 and Fig 4. The Δr(C-H) values are negative at $R_{C...O}$ = 2.7 – 3.5 Å, while they are positive at $R_{C...O}$ ranging from 3.7 to 4.5 Å. This trend is contrasted with a decrease in the C-H stretching frequency as $R_{C...O}$ changing from 2.7 to 4.5 Å. This observation shows that the contraction of the C-H bond, and an increase in the C-H stretching frequency is observed along with a shortening of C···O distance. Fig 4 also points out that at the nearby region of the C···O equilibrium distance ($R_{C...O}$ < 3.9), the change in the C-H stretching frequency in complexes compared to corresponding monomers is more quickly increased as $R_{C...O}$ decreases. Consequently, the closer distance of C···O leads to an increase in the C-H blue shift

https://doi.org/10.62239/jca.2025.023

stretching frequency, and vice versa. The influence of change of intermolecular distance on the blue-shifting of hydrogen bond as fixing two interacted atoms of H and O in the hydrogen bond was reported in the complex of F_3CH with OH_2 [45,46]. In the present work, with another approach, intermolecular distances of C···O are fixed by different values in order to allow H to move more freely between C and O atoms. Thereby, the impact of changes of the C···O distances on those of the C-H bond lengths and its stretching frequencies could be observed more properly. It is found that the tendency in the C-H blue shift rises following the shortening of intermolecular distance between C and O in two isolated monomers.

SAPT2+ analysis

To elucidate the role of factors contributing to the overall stabilization of complexes, energy components were evaluated by employing the SAPT2+ analysis with the 6-311++G(3df,2pd) basis set. The results show that the stability of X_3CH···OC complexes are mainly contributed by three components, including electrostatic, induction and dispersion. Therein, the dispersion component plays the most important role with its energy of -2.8÷-5.3 kJ.mol^{-1} accounting for 43.8% to 45.9%. Meanwhile, the electrostatic and induction terms only account for 30.6-34.5% (E_{ele} = -2.1÷-3.5 kJ.mol^{-1}) and 18.4-19.6% (E_{ind} = -1.1÷2.1 kJ.mol^{-1}), respectively. Therefore, the dispersion and electrostatic components play decisive roles in the stabilization of complexes, in which a larger contribution is observed for the former.

For evaluating the effects of energetic components on complexes stabilization when fixing the different distances of $R_{C...O}$, SAPT2+ analysis for these complexes at the same theory level are performed and the obtained results are gathered in Table S3 and Fig 5. Table S3 shows that all investigated complexes exhibit a decrease in their total energy of components (E_{SAPT2+}), from their positive values at $R_{C...O}$ = 2.7 Å to their minimum energy region at $R_{C...O}$ = 3.3–3,7 Å (E_{SAPT2+} = -1.2÷-4.1 kJ.mol^{-1}), before rising gradually as $R_{C...O}$ ≥ 3.8 Å. Thus, the E_{SAPT2+} of equilibrium geometrical structures of complexes ranging from -2.3 to -4.1 kJ.mol^{-1} also fall into the minimum region of energy. In addition, the percentage of dispersion component increases along with the decrease in the energetic percentage of induction term, during the lengthening of C···O distance. Therefore, at the short intermolecular distance of C···O, the polarity of X_3CH monomers causes a significant induction effect. However, when the intermolecular contact between monomers increases, the effect of induction is gradually surpassed by the dispersion one.

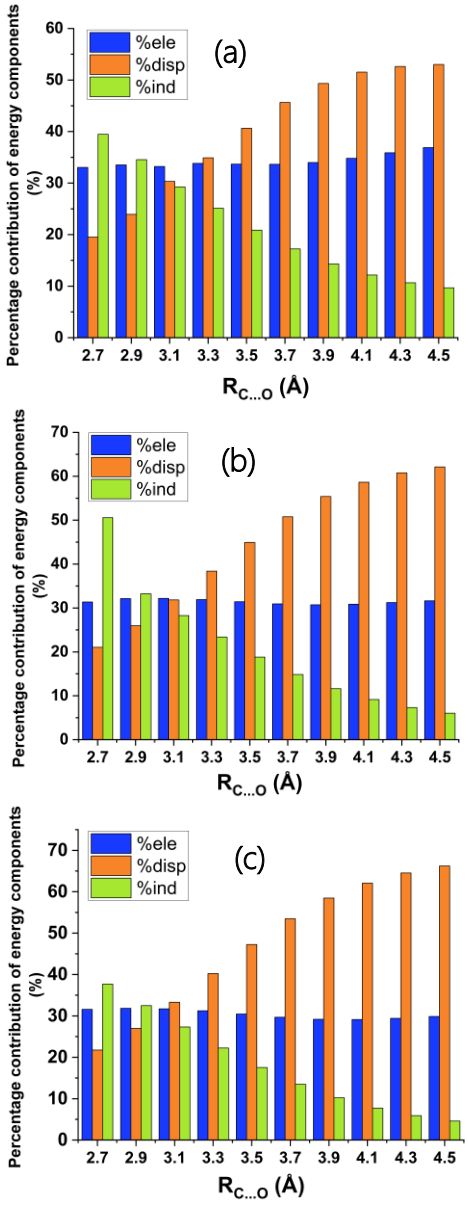

Fig 5. The charts of percentage contribution of energy components (%) to the complex stabilization with the change of C···O distance ($R_{C...O}$, Å) ((a) For F_3CH···OC, (b) For Cl_3CH···OC, (c) For Br_3CH···OC). %elec, %disp,and %ind are in turn abbreviated by distributing percentage of electrostatic, dispersion and induction parts to complex stabilization

As shown in Table S3 and Fig 5 both dispersion and induction energies become less negative as $R_{C...O}$ increases. When $R_{C...O}$ is raised, the exchange term becomes less positive. In addition, for the $R_{C...O}$ = 2.7–3.3 Å, the energy values of the exchange component are much more positive than the sum of electrostatic, induction and dispersion energies. The complexes are thus not stable on the potential surface at $R_{C...O}$ = 2.7–3.3 Å.

https://doi.org/10.62239/jca.2025.023

Remarkably, at the nearby region of equilibrium distance of $R_{C...O}$ from 3.3 Å to 3.7 Å, the decrease in the blue shift of C-H stretching frequency involving C-H···O hydrogen bonds is observed along with an increase in the dispersion component and a decline in the induction one (Figures S1a, and 1b) while the electrostatic has almost no impact.

Conclusion

The interaction energies of stable structures calculated at MP2/6-311++G(3df,2dp) are in the range of -0.6 kJ.mol^{-1} to -2.5 kJ.mol^{-1}. The strength of complexes decreases in the order of Br_3CH···OC > Cl_3CH···OC > F_3CH···OC. The stability of X_3CH···OC complexes is determined by the nonconventional C-H···O hydrogen bond, which is proportional to the polarity of the C-H bond in the X_3CH proton donors.

For $R_{C...O}$ = 3.3– 3.7 Å, the existence of the C-H···O blue shifting hydrogen bonds are observed. The C-H blue shift involving C-H···O hydrogen bond increase in the sequence of substituted derivatives F < Cl < Br, being agreement with the decrease in the occupation at σ^*(C-H) orbital becoming deeper when X goes from F to Br. It is remarkable that a larger percentage of the dispersion relative to the induction and the electrostatic term is observed at the nearby region of equilibrium distance of $R_{C...O}$ from 3.3 Å to 3.7 Å, which corresponds to a contraction and a blue shift of C-H stretching frequency in the C-H···O hydrogen bond.

The SAPT2+ results show that the complex stabilization is contributed by electrostatic, dispersion and induction components, in which, the dispersion term is more dominant in stabilizing complexes, which is up to 46%.

Acknowledgement.

This research was funded by the Vietnam National Foundation for Science and Technology Development (NAFOSTED) under grant number 104.06-2023.49.

References

1. X. Chang, Y. Zhang, X. Weng, P. Su, W. Wu, Y. Mo, J. Phys. Chem. A, 120(17) (2016) 2749–2756. https://doi.org/10.1021/acs.jpca.6b02245
2. G. R. Desiraju, J. Am. Chem. Soc., 135(27) (2013) 9952–9967. https://doi.org/10.1021/ja403264c
3. G. A. Jeffrey, An Introduction to Hydrogen Bond, Oxford University Press, New York (1997).
4. X. Li, L. Liu, H. B. Schlegel, J. Am. Chem. Soc., 124(40) (2002) 9639–9647. https://doi.org/10.1021/ja020213j
5. K. Müller-Dethlefs, P. Hobza, Chem. Rev., 100(1) (2000) 143–167. https://doi.org/10.1021/cr9900331
6. D. J. Philip, J. F. Stoddart, Angew. Chem. Int. Ed., 35(10) (1996) 1154–1196. https://doi.org/10.1002/anie.199611541
7. H.-J. Schneider, Angew. Chem. Int. Ed., 48(21) (2009) 3924–3977. https://doi.org/10.1002/anie.200802947
8. G. A. Jeffrey, W. Saenger, Hydrogen Bonding in Biological Structures, Springer, Berlin Heidelberg (1991).
9. G. R. Desiraju, T. Steiner, The Weak Hydrogen Bond in Structural Chemistry and Biology, Oxford University Press, Oxford (1999).
10. S. Scheiner, Hydrogen Bonding: A Theoretical Perspective, Oxford University Press, New York (1997).
11. L. J. Karas, C. H. Wu, R. Das, J. I. C. Wu, WIREs Comput. Mol. Sci., 10(6) (2020) e1477. https://doi.org/10.1002/wcms.1477
12. J. J. J. Dom, B. U. W. Maes, W. A. Herrebout, B. J. Van der Veken, Chem. Phys. Lett., 469(1–3) (2009) 85–89. https://doi.org/10.1016/j.cplett.2008.12.038
13. Y. Liu, X. Li, C. Qian, S. Müller, K. Skrzyńska, S. Gallego-Parra, … X. Wu, Inorg. Chem., 64(17) (2025) 7570–7579. https://doi.org/10.1021/acs.inorgchem.5c00522
14. I. Gadwal, Macromol., 1(1) (2020) 18–36. https://doi.org/10.3390/macromol1010003
15. J. I. Palacios-Ramírez, L. F. Hernández, A. Pérez-González, A. Galano, F. J. González, ChemElectroChem, (2025) 2500029. https://doi.org/10.1002/celc.202500029
16. L. Pauling, J. Am. Chem. Soc., 53(5) (1931) 1367–1400. https://doi.org/10.1021/ja01355a027
17. G. T. Trudeau, J.-M. Dumas, P. Dupuis, M. Guerin, C. Sandorfy, Van der Waals Syst., 93(??) (1980) 91–123. https://doi.org/10.1007/3-540-10058-X_9
18. K. Hermansson, J. Phys. Chem. A, 106(18) (2002) 4695–4702. https://doi.org/10.1021/jp0143948
19. E. Boldeskul, I. F. Tsymbal, Z. Latajka, A. J. Barnes, J. Mol. Struct., 436–437 (1997) 167–171. https://doi.org/10.1016/S0022-2860(97)00137-3
20. P. Hobza, V. Špirko, Z. Havlas, K. Buchhold, B. Reimann, H. D. Barth, B. Brutschy, Chem. Phys. Lett., 299(2–4) (1999) 180–186. https://doi.org/10.1016/S0009-2614(98)01264-0
21. G. R. Desiraju, Acc. Chem. Res., 24(8) (1991) 290–296. https://doi.org/10.1021/ar00010a002
22. N. T. Trung, T. T. Hue, M. T. Nguyen, Phys. Chem. Chem. Phys., 11(5) (2009) 926–933. https://doi.org/10.1039/B816112G
23. R. Gopi, N. Ramanathan, K. Sundararajan, Chem. Phys., 476 (2016) 36–45. https://doi.org/10.1016/j.chemphys.2016.07.016
24. W. A. Herrebout, S. M. Melikova, S. N. Delanoye, K. S. Rutkowski, D. N. Shchepkin, B. J. van der Veken, J. Phys. Chem. A, 109(14) (2005) 3038–3044. https://doi.org/10.1021/jp0448696
25. A. Mukhopadhyay, M. Mukherjee, P. Pandey, A. K. Samanta, B. Bandyopadhyay, T. Chakraborty, J. Phys. Chem. A, 113(11) (2009) 3078–3087. https://doi.org/10.1021/jp900473w
26. Behera, P. K. Das, J. Phys. Chem. A, 123(8) (2019) 1830–1839. https://doi.org/10.1021/acs.jpca.8b12200

27. R. Szostak, Chem. Phys. Lett., 516 (2011) 166–170. https://doi.org/10.1016/j.cplett.2011.09.082
28. T. T. N. Trang, D. T. Hien, T. N. Trung, P. N. Hung, K. P. Duy, T. T. Hue, Vietnam J. Chem., 48(4C) (2010) 329–334.
29. N. T. Thi Hong Man, P. Le Nhan, V. Vo, D. T. Tuan Quang, N. T. Tien Trung, Int. J. Quantum Chem., 117(5) (2016) e25338. https://doi.org/10.1002/qua.25338
30. N. T. Tri, N. T. H. Man, N. Le Tuan, N. T. T. Trang, D. T. Quang, N. T. Trung, Theor. Chem. Acc., 136(1) (2016) 10. https://doi.org/10.1007/s00214-016-2032-4
31. L. T. T. Quyen, N. T. Trung, RSC Adv., 14(70) (2024) 40018–40030. https://doi.org/10.1039/D4RA07498J
32. N. T. Trung, T. T. Huế, N. M. Thọ, Vietnam J. Chem., 45(4) (2007) 685–685. https://doi.org/10.15625/4814
33. S. Scheiner, T. Kar, J. Phys. Chem. A, 106(8) (2002) 1784–1789. https://doi.org/10.1021/jp013702z
34. M. J. Frisch, G. W. Trucks, H. B. Schlegel, G. E. Scuseria, M. A. Robb, J. R. Cheeseman, G. Scalmani, V. Barone, B. Mennucci, G. Petersson, Gaussian 09, Revision D.01; Gaussian, Inc.: Wallingford, CT (2009).
35. S. F. Boys, F. Bernardi, Mol. Phys., 19(6) (1970) 553–566. https://doi.org/10.1080/00268977000101561
36. R. F. W. Bader, Atoms in Molecules: A Quantum Theory, Oxford University Press, UK (1990).
37. R. F. W. Bader, Acc. Chem. Res., 8(1) (1985) 9–15. https://doi.org/10.1021/ar00109a003
38. E. Espinosa, E. Molins, C. Lecomte, Chem. Phys. Lett., 285(3–4) (1998) 170–173. https://doi.org/10.1016/S0009-2614(98)00036-0
39. F. Weinhold, E. D. Glendening, NBO 5.0 program manual, Theoretical Chemistry Institute, University of Wisconsin, Madison, WI (2001).
40. J. Misquitta, R. Podeszwa, B. Jeziorski, K. Szalewicz, J. Chem. Phys., 123(21) (2005) 214103. https://doi.org/10.1063/1.2135288
41. I.Alkorta, I. Rozas, J. Elguero, Chem. Soc. Rev., 27(2) (1998) 163–170. https://doi.org/10.1039/A827163Z
42. W. Zierkiewicz, P. Jurečka, P. Hobza, ChemPhysChem, 6(4) (2005) 609–617. https://doi.org/10.1002/cphc.200400243
43. F. Vilela, P. R. Barreto, R. Gargano, C. R. Cunha, Chem. Phys. Lett., 427(1–3) (2006) 29–34. https://doi.org/10.1016/j.cplett.2006.06.040
44. V. Alabugin, M. Manoharan, S. Peabody, F. Weinhold, J. Am. Chem. Soc., 125(19) (2003) 5973–5987. https://doi.org/10.1021/ja034656e
45. J. Joseph, E. D. Jemmis, J. Am. Chem. Soc., 129(15) (2007) 4620–4632. https://doi.org/10.1021/ja067545z
46. Y. Mao, M. Head-Gordon, J. Phys. Chem. Lett., 10(14) (2019) 3899–3905. https://doi.org/10.1021/acs.jpclett.9b01203